www.nature.com/cr
www.cell-research.com

Cell Research

LETTER TO THE EDITOR

Optogenetic gene editing in regional skin

Cell Research (2019) 29:862–865; https://doi.org/10.1038/s41422-019-0209-9

Dear Editor,

Significant breakthrough in science often relies on the development of original tools that can perform novel functions, thus help reveal previously unknown knowledge that is not feasible to obtain using conventional tools or methods. Genetic manipulation has become a standard practice in almost all biological research fields; consequently gene expression control systems such as Cre and rtTA are indispensable tools for biomedical studies.[1,2] Inducible systems of the standard gene regulation tools are controlled by addition of freely diffusible small molecules such as an antibiotic or a steroid analogue.[1–3] However, the growing complexity of scientific research requires the development of more precise gene regulation systems that can spatiotemporally control gene expression in a tunable and reversible manner. In comparison to chemical agents, light is an ideal inducer of gene expression in a spatiotemporal specific manner. Optogenetic tools have revolutionized the studies in neuroscience and are quickly changing the standard practice in many other fields.[4–9] These systems utilize light sensitive proteins to facilitate spatiotemporal protein activation, localization or genetic alterations. However, most of the light-controlled gene regulation systems were established and applied in vitro, while in vivo light switchable gene regulation system still remains a major unmet biomedical research need. A novel optogenetic mouse system that could enable spatiotemporal gene manipulations in vivo will facilitate novel discoveries.

To generate a novel genetic tool that will enable in vivo spatiotemporal specific gene manipulation, we designed a new light activated rtTA (Li-rtTA) system by utilizing the *Arabidopsis thaliana* light-sensitive protein cryptochrome 2 (CRY2) and its binding partner CIB1protein[7,10] (Fig. 1a). Conventional rtTA contains two functional domains: the DNA binding domain rTetR that binds to the tetracycline response element (TRE) in the presence of doxycycline, and the trans-activation domain VP16 that is a transcriptional activation domain from herpes simplex virus.[1] Our rationale is that by separating these two domains of rtTA and fusing them respectively to the light sensitive protein CRY2 and CIB1, we will be able to reunite them under condition of region-specific light activation *via* dimeratization of the CRY2 and CIB1. Then in the presence of doxycyline the united two components of rtTA will be able to bind TRE and drive downstream gene expression similar to an intact rtTA. There are several advantages to this design: (1) The dual control of light activation and doxycycline will ensure tight spatiotemporal specific gene manipulation; (2) By using rtTA as the light-activated module we will be able to utilize many existing genetic tools to achieve diverse spatiotemporal utilities; (3) The activation of gene expression is reversible, if not involving genomic DNA deletion.

To test our theory and identify the most effective fusion protein combination, we designed several different versions of Li-rtTA. Based on previous results regarding the function and efficiency of CIB1 and CRY2 proteins,[7] we generated a series of constructs comprising rTetR fused to either full-length CIB1 or truncated versions of the N-terminus of CIB1(CIBN) (*CIB1-rTetR-CIB1* or *CIBN-rTetR-CIBN*); we also generated different versions of VP16 fused to either full-length CRY2(CRY2FL) or a truncated CRY2(CRY2PHR) that only contains the CRY2's photolyase homology region (*CRY2FL-VP16* or *CRY2PHR-VP16*). To test the efficiency of our constructs we transfected these constructs into keratinocytes expressing *TetO-H2BGFP*, which will express GFP with functional rtTA in the presence of doxycycline (Fig. 1b). Our results showed the combination of CRY2PHR-VP16 with CIBN-rTetR-CIBN achieved the highest induction efficiency with light illumination and doxycycline treatment. Most importantly it is not leaky with either blue light illumination or doxycycline treatment alone (Fig. 1c). Next these two constructs were cloned into a single vector linked by a 2A sequence with different orders: *CIBN-rTetR-CIBN-2A-CRY2PHR-VP16*, or *CRY2PHR-VP16-2A-CIBN-rTetR-CIBN* (Supplementary information, Fig. S1a). We then separately transfected both plasmids into keratinocytes expressing reporter *TetO-H2BGFP* to compare their induction efficiency. Western blot analysis showed the *CIBN-rTetR-CIBN-2A-CRY2PHR-VP16* construct express equal levels of the two components, as compared to separate transfection of individual plasmid (Supplementary information, Fig. S1b). And the *CIBN-rTetR-CIBN-2A-CRY2PHR-VP16* construct also showed higher induction efficiency than *CRY2PHR-VP16-2A-CIBN-rTetR-CIBN* construct (Supplementary information, Fig. S1c). Therefore, *CIBN-rTetR-CIBN-2A-CRY2PHR-VP16* was selected as the optimal design used for further study and was named Li-rtTA.

Next we tested two essential features of our Li-rtTA: first its ability to reversibly activate gene expression. To do this, we established a *Li-rtTA::TetO-luciferase* keratinocyte cell line and monitored luciferase activity during cyclic blue light and darkness treatment, in the presence of doxycycline. We measured the luciferase activity at interval time points and found that luciferase expression level increased with the treatment of blue light illumination, then it decreased and dropped back to the base line level after switching back to darkness. Subsequent light and darkness treatment induced the same cyclic expression pattern of the luciferase activity (Fig. 1d). This clearly demonstrates the reversible gene activation of our Li-rtTA system. Secondly, we tested its ability of spatiotemporal specific gene induction. For this we used the *Li-rtTA::TetO-H2BGFP* keratinocyte cell line. A time-lapse live imaging experiment revealed that H2BGFP expression started as early as 3 h after light illumination (Supplementary information, Fig. S1d). Then a confluent cell culture of *Li-rtTA::TetO-H2BGFP* keratinocytes was illuminated with blue light from the bottom of petri dish through a 3D printed photomask with engraved letters "NIBS" in the middle (Supplementary information, Fig. S1e). In the presence of doxycycline, after 12 h of illumination only the regions exposed to blue light expressed H2BGFP, giving rise to a clear fluorescent pattern of "NIBS" in the culture (Fig. 1e). These results confirmed the successful construction of our Li-rtTA system that is capable of reversible and spatiotemporal specific gene manipulation in vitro.

To utilize this tool for spatiotemporal gene manipulation in vivo, we used CRISPR/Cas9 to insert the Li-rtTA expression cassette into

Received: 24 April 2019 Accepted: 8 July 2019
Published online: 31 July 2019

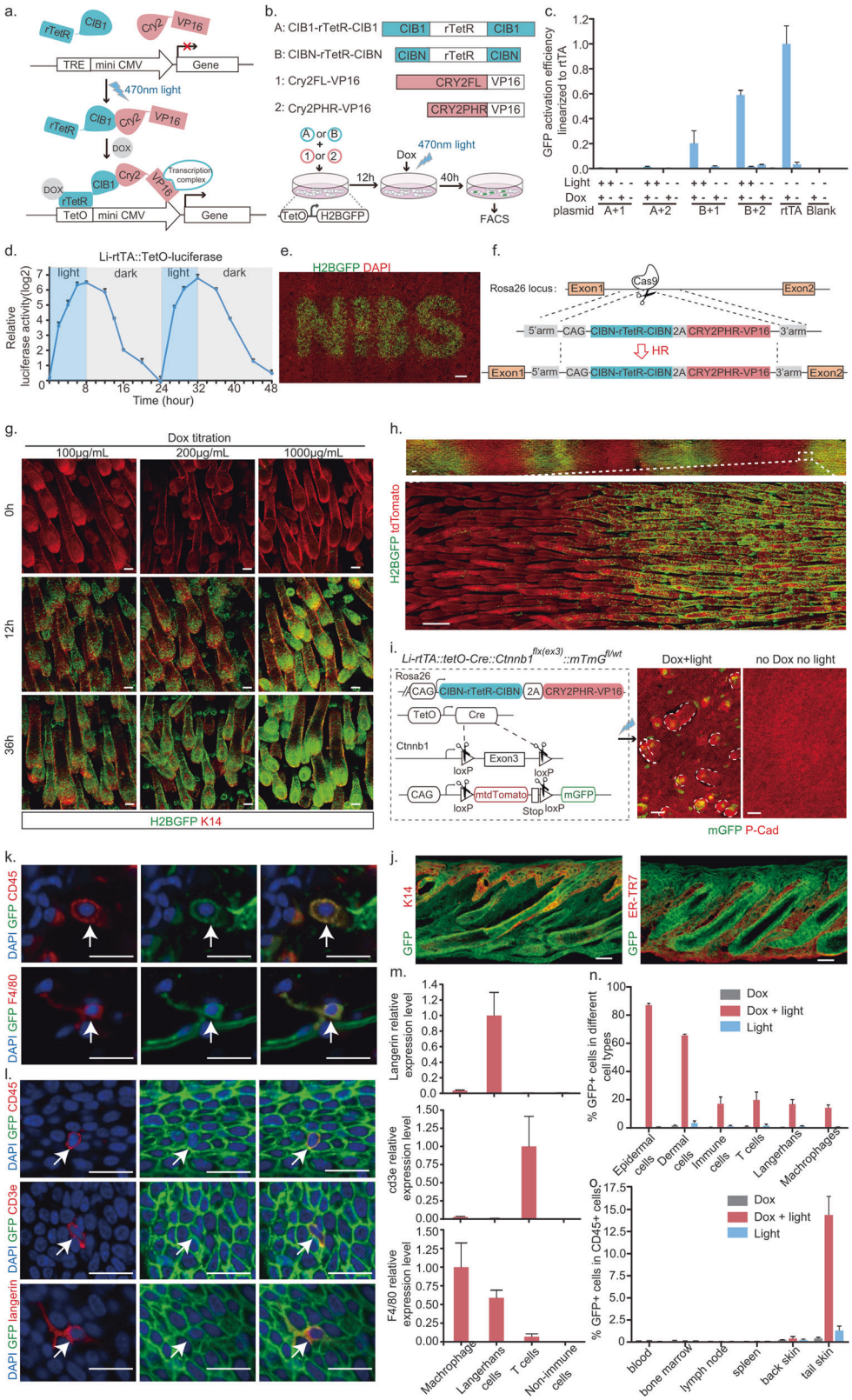

intron one of the *Rosa26* gene (Fig. 1f). This will ensure ubiquitous expression of Li-rtTA and the feasibility of spatiotemporal gene manipulation in any cell types in vivo. Successful knock-in was confirmed by genotyping and sequencing (Supplementary information, Fig. S2a–c). The induction specificity of Li-rtTA was determined by using the *Li-rtTA::TetO-H2BGFP* mice (Supplementary information, Fig. S2d). Mice kept in darkness did not express H2BGFP, even in the presence of increasing concentration of

Fig. 1 Novel optogenetic tool Li-rtTA enables spatiotemporal specific gene activation and deletion in vivo. **a** Schematic diagram of the working theory of Light-rtTA (Li-rtTA) system. The two functional domains of rtTA, DNA binding domain rTerR and transactivation domain VP16, were separated and linked to light sensitive proteins CIB1 and Cry2 respectively. Blue light with wavelength of 470 nm stimulates dimerization of CRY2 and CIB1, thus bringing rTetR and VP16 together to function as an intact rtTA. In the presence of doxycycline, the dimerized fusion proteins will activate Tet-On system and drive downstream gene expression. Under the dual control of blue light and doxycycline, Li-rtTA system can achieve spatiotemporal specific gene manipulation. **b** Schematic diagram of Li-rtTA constructs optimization. rTetR and VP16 were individually fused to CIB1 and Cry2 with different lengths. Then different combination of these two components were transfected into keratinocytes expressing reporter gene TetO-H2BGFP to evaluate their efficiency. Percentage of GFP+ cells were quantified by FACS. **c** Activation efficiency of Li-rtTA system with different constructs combination as illustrated in **b**. Conventional rtTA was used as a positive control. All results were normalized to rtTA activation efficiency. The presence or absence of blue light / doxycycline were used to evaluate the leakiness of the system. **d** Temporally controlled and reversible gene activation achieved by Li-rtTA. Keratinocytes stably express optimized Li-rtTA and reporter gene TetO-Luciferase. In the presence of doxycycline, dynamic expressions of luciferase under the control of Li-rtTA during cyclic blue light and darkness treatment were recorded. **e** Spatially controlled gene activation by Li-rtTA. Keratinocytes expressing Li-rtTA and TetO-H2BGFP were illuminated from the petri dish bottom through a black photomask with the engraved "NIBS" pattern, as illustrated in Supplementary information, Fig. S1e. In the presence of doxycycline, only the light-permeated region gave rise to GFP+ NIBS letters in the culture. Scale bar = 1 mm. **f** Schematic diagram of CRISPR/Cas9 mediated knock-in of Li-rtTA cassette at the *Rosa26* locus. *CIBN-rTetR-CIBN* and *CRY2PHR-VP16* is linked by a *2A* sequence. **g** Blue light- and doxycycline- dependent activation of gene expression in the *Li-rtTA* knock-in mice. *Li-rtTA::TetO-H2BGFP* mice were treated with indicated conditions of increasing amount of doxycycline and light activation time, as illustrated in Supplementary information, Fig. S2d. Representative wholemount immunofluorescence images reveal H2BGFP expression pattern in tail skin epithelium after indicated treatments. K14 is a marker for epithelium cells. Scale bars = 50 μm. **h** In vivo spatiotemporal specific gene activation controlled by the Li-rtTA system in *Li-rtTA::TetO-H2BGFP::mTmG* mice, as illustrated in Supplementary information, Fig. S2f. In the presence of doxycycline, only the blue light-exposed skin regions express strips of GFP+ cells in the tail skin epithelium, indicating spatial specific gene activation using Li-rtTA in vivo. Scale bars = 200 μm. **i** In vivo genetic deletion controlled by the Li-rtTA system in *Li-rtTA::TetO-Cre::Ctnnb1*$^{flx(ex3)}$*::mTmG* mice. Left panel, schematic diagram of in vivo genetic deletion of LoxP flanked *Ctnnb1* exon3 and *membrane Tomato-stop* genetic loci using Li-rtTA system. Right panel, stabilization of beta-catenin after exon3 deletion results in de novo hair follicle-like structure formation in ventral plantar hind paw skin. Reporter gene mGFP expression also indicates Li-rtTA induced Cre activity in vivo. Scale bars = 50 μm. **j** Representative section immunofluorescence images of tail skin in *Li-rtTA::TetO-Cre::mTmG* mice after the treatment illustrated in Supplementary information, Fig. S4a. Li-rtTA-dependent Cre expression excises LoxP flanked *membrane-Tomato-stop* cassette to allow reporter gene *membrane-GFP* expression. Both epithelial cells (marked by K14 staining) and dermal cells (marked by ER-TR7 staining) express membrane GFP, indicating activation of the Li-rtTA in vivo in both skin layers after the treatment. Scale bars = 50 μm. **k** Representative whole mount immunofluorescence images of tail skin dermis in *Li-rtTA::TetO-Cre::mTmG* mice after the treatment illustrated in Supplementary information, Fig. S4a. Various dermis resident immune cells were labeled with specific markers: F4/80 for macrophage, and CD45 for immune cells. Scale bars = 20 μm. **l** Representative whole mount immunofluorescence images of tail skin epidermis in *Li-rtTA::TetO-Cre::mTmG* mice after the treatment illustrated in Supplementary information, Fig. S4a. Various epidermis resident immune cells were labeled with specific markers: langerin for langerhan cells, CD3e for T cells, and CD45 for immune cells. Co-expressions of immune cell markers and membrane GFP indicate efficiently genetic labeling of skin resident immune cells in *Li-rtTA::TetO-Cre::mTmG* mice. Scale bars = 20 μm. **m** Validation of different FACS-isolated immune cell types using qPCR. Langerin is a Langerhan cell marker gene. Cd3e is a T cell marker gene. F4/80 is a macrophage marker gene. **n** FACS quantification of %GFP+ cells reveals genetic labeling efficiency of different cells types in light exposed tail skin using *Li-rtTA::TetO-Cre::mTmG* mice. Mice treated with doxycycline only and light only served as control. **o** In vivo spatiotemporal specific genetic labeling of resident immune cells in regional skin using *Li-rtTA::TetO-Cre::mTmG* mice. FACS quantification of % GFP+ cells reveals genetic labeling efficiency of immune cells isolated from tail skin and other organs shielded from light illumination in *Li-rtTA::TetO-Cre::mTmG* mice. Mice treated with doxycycline only and light only served as control. Note only immune cells isolated from light exposed skin regions were genetically labeled with GFP expression

doxycycline (Fig. 1g). This indicates strict blue light dependent activation of Li-rtTA. In the presence of doxycycline, prolonged blue light illumination leads to higher H2BGFP expression in vivo (Fig. 1g, Supplementary information, Fig. S2e). Next, we tested the ability of our Li-rtTA to achieve spatiotemporal gene activation in vivo. For this we used *Li-rtTA::TetO-H2BGFP::mTmG* mice. The mTmG allele was used to label all cells with membrane Tomato to facilitate wholemount imaging. To block light exposure at specific regions, mouse tail was painted with strips of black nail polish. Then mice were exposed to blue light illumination and doxycycline (Supplementary information, Fig. S2f). After treatment, only light exposed skin regions expressed abundant H2BGFP. The clear strip pattern of H2BGFP expression in tail skin of the *Li-rtTA::tetO-H2BGFP::mTmG* mice indicates stringent spatiotemporal gene activation of our Li-rtTA system in vivo (Fig. 1h).

The above results demonstrate that we could activate gene expression at a spatiotemporal specific manner in vivo using our Li-rtTA mice. A unique advantage of this system is that we can utilize many existing genetic tools to achieve diverse spatiotemporal gene manipulations. For instance, besides gene activation, we can also achieve spatiotemporal specific gene deletion by using the TetO-Cre. To test this ability, we used the *Li-rtTA::TetO-Cre::mTmG* mice. Li-rtTA induced expression of Cre will delete *loxP* flanked *mTomato-stop* and allow *mGFP* expression. This will label light activated cells and all their progenies membrane GFP+. Whole body exposure to blue light in the presence of doxycycline efficiently labeled skin epidermis and dermis mGFP+ in both back and tail skin, while doxycycline only or blue light only treated mice did not result in any labeling (Supplementary information, Fig. S3a, b). We also tested whether our Li-rtTA can be used to genetically label cells in internal organs using *Li-rtTA::TetO-Cre::mTmG* mice. Blue light can penetrate skin with whole body light exposure, and internal organs such as heart, liver, spleen, lung, and kidney, show effective expression of GFP (Supplementary information, Fig. S3c). These labeling are also dependent on dual control of blue light and doxycycline, because neither treatment alone can induce genetic labeling in these internal organs (Supplementary information, Fig. S3c). This indicates light dependent activation of our Li-rtTA system can be used to genetically label cells in multiple organs in vivo.

To further test the ability of our Li-rtTA induced expression of Cre to genetically delete an endogenous gene locus and cause physiological phenotype, we employed the *Li-rtTA::TetO-Cre::Ctnnb1flx(exon3)::mTmG* mice (Fig. 1i, Supplementary information, Fig. S3d). Conditional deletion of exon3 from *Ctnnb1* leads to stabilized beta-catenin and activation of Wnt signaling, which can initiate de novo hair follicle branch formation.[11] There are no hair follicles on ventral plantar hind paw skin, so we chose this skin region for our assay. The hind paw of P6 mice were treated with blue light illumination in the presence of doxycycline for 6 h (Supplementary information, Fig. S3e). 15 days post treatment, de novo hair follicle like structure was induced in ventral plantar hind

paw skin, while no doxycycline and no light treatment control group didn't generate any such structures (Fig. 1i). These results convincingly demonstrated the ability of our Li-rtTA system to achieve genomic DNA deletion in a spatiotemporal manner in vivo.

Skin is the first line of defense of an animal's body against the environment. It is a complex organ containing many different and essential cell types: epithelial cells, dermal cells and immune cells etc.[12] To test the full spectrum of cells that can be labeled within mouse skin, we use the *Li-rtTA::TetO-Cre::mTmG* mice. Mice tail skin was treated with blue light illumination and doxycycline (Supplementary information, Fig. S4a). Upon close examination, our light-induced genetic labeling is able to mark all of the major cell types in skin. These include Keratin14$^+$ epithelial cells, ER-TR7$^+$ dermal fibroblasts, CD45$^+$ immune cells in both epidermis and dermis, CD3e$^+$ T cells in epidermis, Langerin$^+$ Langerhans cells in epidermis, and F4/80$^+$ macrophages in dermis (Fig. 1j–l). None of these cells were labeled with doxycycline only or light only treatment (Supplementary information, Fig. S3f).

Next to stringently test the fidelity of spatiotemporal specific genetic labeling of cells in regional skin, we use the *Li-rtTA::TetO-Cre::mTmG* mice to specifically label different cells types in tail skin only. Then we analyzed the labeling efficiency of various cell populations in both light illuminated region and non-illuminated regions, such as adjacent back skin and internal organs (Supplementary information, Fig. S4a). We used FACS to quantify the labeling efficiency of immune cells from different regions: CD45$^+$ to identify total immune cells, CD45$^+$ Langerin$^+$ to identify Langerhans cells, CD45$^+$ CD3e$^+$ to identify T cells, and CD45$^+$ F4/80$^+$ CD64$^+$ to identify macrophages (Supplementary information, Fig. S4b–e). The specificity of the immune cell isolated using our FACS strategy was validated by qPCR analysis of cell type specific markers (Fig. 1m). Using the FACS analysis, we quantified GFP labeling efficiency of different cells types in tail skin treated with blue light illumination and doxycycline, or doxycycline/light alone (Fig. 1n). Among different cell types, epidermal cells showed the highest labeling efficiency of 90%. Next are dermal cells, mostly composed of dermal fibroblasts, which have a labeling efficiency of more than 60%. All of the tail skin immune cells showed lower but consistent labeling efficiency of ~12%. In the doxycycline only or light only control group, none of these cell types showed detectible labeling, consistent with our section staining analysis.

To test the spatiotemporal specific genetic labeling of skin resident immune cells in regional skin, we analyzed labeling efficiency of immune cells isolated from light exposed tail skin and other light shielded organs, such as bone marrow, blood, spleen, lymph node, and dorsal skin. Only tail skin contains GFP+ immune cells, while tissues from the light shielded region such as back skin, lymph node, blood, spleen, and bone marrow did not contain detectible GFP+ immune cells (Fig. 1o, Supplementary information, Fig. S4f–j). In the doxycycline only or light only control group, no or very low level of GFP+ immune cells were detected in tail skin and other light shielded organs.

Together these results demonstrate that our Li-rtTA can genetically label multiple cell types in regional skin in spatiotemporal specific manner. This will enable lineage tracing of different cells in regional skin during regeneration, wounding healing, immune response and other homeostatic or pathological conditions.

ACKNOWLEDGEMENTS

This work was supported by grants from the National Key R&D Program of China (2017YFA0103500) and the National Basic Research Program of China 973 Programs (2012CB518700 and 2014CB849602). We are grateful to the NIBS Animal Facility for their expert handling and care of mice, the NIBS Transgenic Animal Center for generation of knock-in mice, the NIBS Biological Resource Centre for FACS, the NIBS imaging facility for assistance with the confocal microscope experiment. We thank all members of the Chen lab for discussions and technical support.

AUTHOR CONTRIBUTIONS

T.C. and F.L. conceived the project, designed the experiments, and wrote the manuscript. F.L. and Z.L. performed most experiments. F.W. generated CRISPR/Cas9-mediated knock-in mouse. W.W. contributed to plasmid construct. N.Q. contributed to wholemount staining experiments.

ADDITIONAL INFORMATION

Supplementary information accompanies this paper at https://doi.org/10.1038/s41422-019-0209-9.

Competing interests: The authors declare no competing interests.

Fei Li[1,2], Zhiwei Lu[1,2], Wenbo Wu[2], Nannan Qian[2], Fengchao Wang[2] and Ting Chen[2,3]

[1]Graduate School of Peking Union Medical College, Beijing 100871, China; [2]National Institute of Biological Sciences, Beijing 102206, China and [3]Tsinghua Institute of Multidisciplinary Biomedical Research, Tsinghua University, Beijing 100871, China

These authors contributed equally: Fei Li, Zhiwei Lu

Correspondence: Ting Chen (chenting@nibs.ac.cn)

REFERENCES

1. Gossen, M. et al. *Science* **268**, 1766–1769 (1995).
2. Schwenk, F., Baron, U. & Rajewsky, K. *Nucleic Acids Res.* **23**, 5080–5081 (1995).
3. No, D., Yao, T. P. & Evans, R. M. *Proc. Natl Acad. Sci. USA* **93**, 3346–3351 (1996).
4. Deisseroth, K. *Nat. Methods* **8**, 26–29 (2010).
5. Levskaya, A., Weiner, O. D., Lim, W. A. & Voigt, C. A. *Nature* **461**, 997–1001 (2009).
6. Müller, K. & Weber, W. *Mol. Biosyst.* **9**, 596–608 (2013).
7. Konermann, S. et al. *Nature* **500**, 472–476 (2013).
8. Polstein, L. R. & Gersbach, C. A. *Nat. Chem. Biol.* **11**, 198–200 (2015).
9. Yazawa, M., Sadaghiani, A. M., Hsueh, B. & Dolmetsch, R. E. *Nat. Biotechnol.* **27**, 941–945 (2009).
10. Liu, H. et al. *Science* **322**, 1535–1539 (2008).
11. Xu, Z. et al. *Elife* **4**, e10567 (2015).
12. Matejuk, A. *Arch. Immunol. Ther. Exp.* **66**, 45–54 (2018).